

Age models for pelagites and turbidites from the Cap Timiris Canyon off Mauritania

Katharina Wien *, Christine Holz, Martin Kölling, Horst D. Schulz

FB 5 Department of Geosciences, University of Bremen, P.O. Box 330440, 28334 Bremen, Germany

Received 19 February 2005; received in revised form 10 October 2005; accepted 19 October 2005

Abstract

This study of sediments from the Cap Timiris Canyon demonstrates that geochemical data can provide reliable age-depth correlation even of highly turbiditic cores and attempts to improve our understanding of how turbidite emplacement is linked to climatic-related sea-level changes. The canyon incises the continental margin off NW Africa and is an active conduit for turbidity currents. In sediment cores from levee and intrachannel sites turbidites make up 6–42% of sediment columns. Age models were fitted to all studied cores by correlating downcore element data to dated reference cores, once turbidite beds had been removed from the dataset. These age models enabled us to determine turbidite emplacement times. The Cap Timiris Canyon has been active at least over the last 245 kyr, with turbidite deposition seemingly linked to stage boundaries and glacial stages. The highly turbiditic core from the intrachannel site postdates to ≈ 15 kyr and comprises Holocene and late Pleistocene sediments. Turbidite deposition at this site was associated especially with the rapid sea-level rise at the Pleistocene/Holocene transition. During the Holocene, turbidity current activity decreased but did not cease.

© 2005 Elsevier Ltd. All rights reserved.

Keywords: Submarine canyons; Turbidites; Sea-level

1. Introduction

Submarine canyon systems are common on ocean margins and are conduits for channelised mass transport mainly in form of turbidity currents. The resulting depositional pattern is characterised by pelagic sediments interbedded with turbidites (e.g. Bouma, 1962; 2000; Stow and Shanmugam, 1980; Bouma et al., 1985). Various types of turbidite deposition during the Pleistocene and Holocene can be observed along the NW African continental margin (e.g. Simm et al., 1991; Weaver et al., 1992; Masson, 1994; Wynn et al., 2000a,b; 2002), along the NE Atlantic margin (e.g. Davies et al., 1997; Weaver et al., 2000), in the Mediterranean Sea (e.g. Rothwell et al., 1998; 2000; Reeder et al., 2000), or in large turbidite systems such as the Amazon Fan (e.g. Lopez, 2001), the Bengal Fan (e.g. Weber et al., 1997; 2003) and the Zaire Fan (e.g. Babonneau et al., 2002; Droz et al., 2003).

Age dating of these sediments is necessary to obtain information on depositional frequency and emplacement

times of the turbidites. However, conventional methods such as oxygen isotope ($\delta^{18}\text{O}$) analyses, radiocarbon dating or biostratigraphy are time-consuming and expensive, and indirect dating methods such as geochemical correlation are desirable as tools to fit age models. Pearce and Jarvis (1995), for example, used metre-thick turbidites from the Madeira Abyssal Plain off Morocco as geochemical marker beds and correlated them over distances of > 500 km. The intervening centimetre-thick pelagites were assigned to their corresponding oxygen isotope stages (OISs) based on biostratigraphy.

The main purpose of this paper is to show that geochemical correlation of pelagic sequences can be applied to sediment cores which contain from 6 to 42% turbidite layers, and that it is possible to fit age models to these cores by correlation. Cores from the Cap Timiris Canyon in the Atlantic Ocean off Mauritania (Krastel et al., 2004) are suitable to introduce this new method. The canyon was discovered during RV Meteor cruise M 58-1 in April/May 2003 and investigated by combined employment of seismo-acoustic, sedimentological and geochemical techniques (Schulz and Cruise Participants, 2003). In this study, we primarily present geochemical data from four sites in the Cap Timiris Canyon, three of which are located on levee structures and one from the interior part of the channel, where sediment was accumulating.

* Corresponding author. Tel.: +49 421 218 8941; fax: +49 421 218 4321.
E-mail address: kwien@uni-bremen.de (K. Wien).

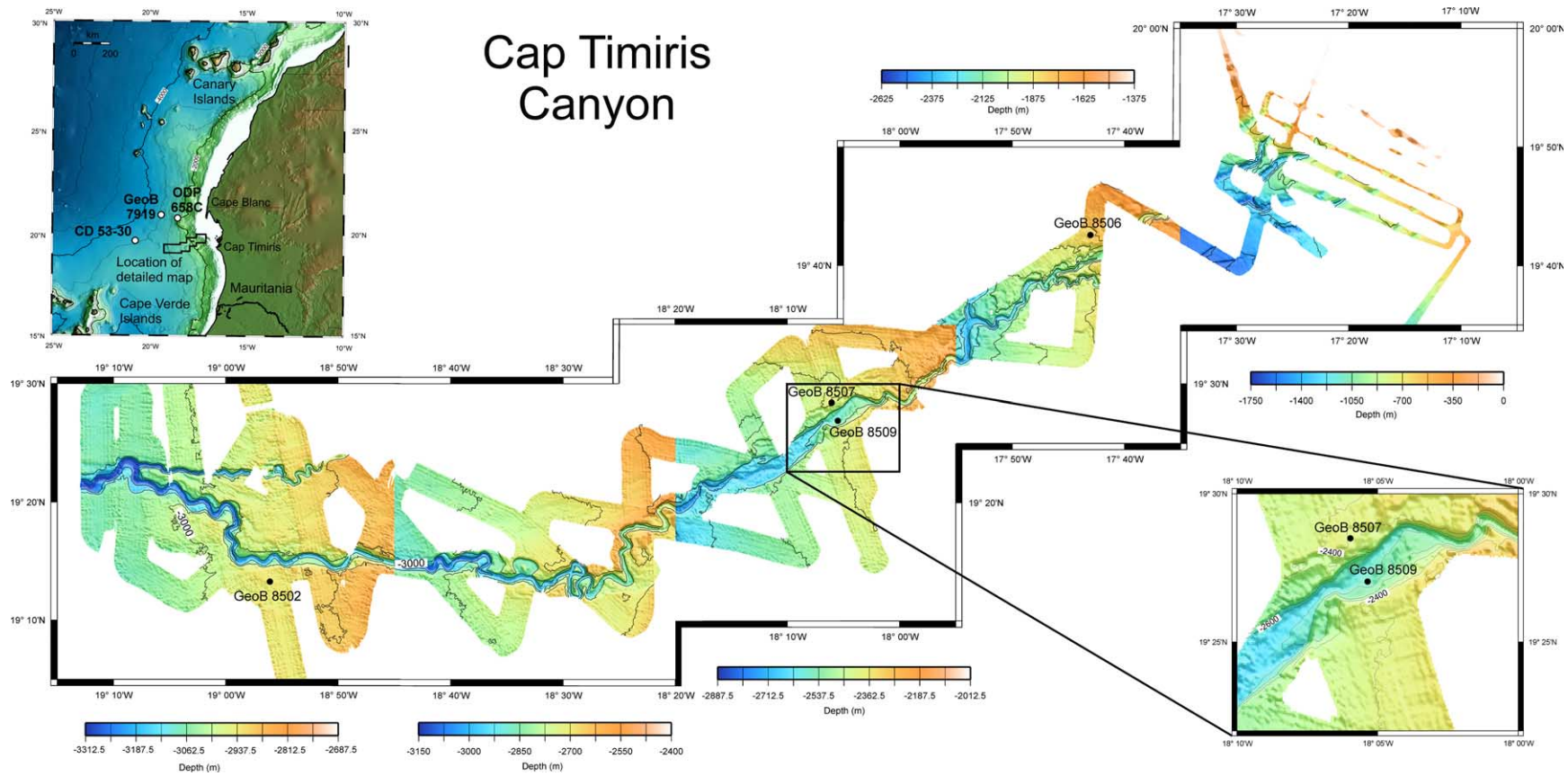


Fig. 1. Overview of the study area. Upper left: general map of the Atlantic Ocean offshore NW Africa with locations of the reference cores (open circles) GeoB 7919-5 (Meggers and Cruise Participants, 2003), CD 53-30 (Matthewson et al., 1995) and ODP 658C (Ruddiman et al., 1988). Main map: locations of selected coring positions (closed circles) in the Cap Timiris Canyon during RV Meteor cruise M 58-1 (this study). Lower right: close-up view of the intra-channel site GeoB 8509 and the adjacent site GeoB 8507 on the northern levee. Slightly modified from Krastel et al. (2004).

In our approach we created age models for the pelagic sequences in all cores based on their downcore element variations. These were correlated to well-dated variations of the carbonate content in two dated reference records obtained from literature. The age models provide information on frequency and emplacement times of turbidites and hence contribute to our understanding of, and quantify, the processes of turbidity-current generation. Main objectives of this paper are.

- (1) to introduce a method for core-to-core correlation using geochemical data on turbidite-containing cores, and
- (2) to determine turbidite emplacement times in the cores and assess emplacement to sea-level stand and climatic conditions.

2. Study site

The Cap Timiris Canyon is an example of an active canyon system off the Mauritanian coast which incises the NW African shelf and continental slope (Krastel et al., 2004). The canyon head abuts the topography-deduced Tamanrasset River System which, although not discharging under present-day climatic conditions, ranks among the largest river systems worldwide. The mouth of this potential river system is located off Cap Timiris whereas its flow pathways, as postulated by Vörösmarty et al. (2000), are now covered by extensive Saharan sand dunes. For the Western Sahara Desert in Mauritania, Lancaster et al. (2002) describe three main periods of dune generation from 25–15, 13–10 kyr and after 5 kyr.

The dunes may relate to the Pleistocene/Holocene history of the Tamanrasset River System in that they covered its flow pathways (as is the case today) and accumulated considerable amounts of sand in dry river beds (wadis). This material may have been transported episodically into the ocean, and thereby into the Cap Timiris Canyon, during flash floods.

Channelised gravity-driven mass transport processes deliver sediment from the shelf and upper continental slope to the deep-sea abyssal plain. Today sediment feeding into the canyon mainly derives from eolian dust from the sub-Sahara and Sahel region (Tetzlaff and Wolter, 1980; Pye, 1987; Wefer and Fischer, 1993) and from intensive biomass production due to upwelling, especially in the proximal parts of the canyon (e.g. Fütterer, 1983; Bertrand et al., 1996; Martinez et al., 1999). Upwelling activity is considered to generally have been most intense during glacial conditions (Diester-Haass and Chamley, 1982). Terrigenous input likewise increased during glacial periods, mainly due to enhanced availability of source material and strength of transporting winds (Matthewson et al., 1995; deMenocal et al., 2000).

3. Materials

In this study, geochemical analyses were performed onboard during RV Meteor cruise M 58-1 in April/May 2003 (Schulz and Cruise Participants, 2003) on four gravity cores and their corresponding multicorer cores (MUCs) from the Cap Timiris Canyon (Fig. 1 and Table 1). Three of these coring sites are on levee structures (GeoB 8502, GeoB 8506, GeoB 8507) and one at an intrachannel location (GeoB 8509). GeoB 8502 is a pelagic site in the lower reaches of the canyon whereas sites

Table 1

Key parameters of cores discussed in this study including core number, geographic position, water depth, location in the canyon system, gear type, recovery and available data

Core no.	Latitude (N)	Longitude (W)	Water depth (m)	Location in canyon system	Gear type	Recovery (cm)	Available data
Cores from the Cap Timiris Canyon							
GeoB 8502-4	19°13.21'	18°56.05'	2952	Levee	MUC	24	XRF; shipboard
GeoB 8502-2	19°13.27'	18°56.04'	2956	Levee	GC	1478	XRF; shipboard
GeoB 8506-1	19°42.56'	17°42.94'	1828	Levee	MUC	30	XRF; shipboard
GeoB 8506-2	19°42.57'	17°42.95'	1827	Levee	GC	1008	XRF; shipboard
GeoB 8507-1	19°28.49'	18°05.97'	2414	Levee	MUC	34	XRF; shipboard
GeoB 8507-3	19°28.50'	18°05.97'	2411	Levee	GC	1000	XRF; shipboard
GeoB 8509-3	19°27.01'	18°05.34'	2584	Intrachannel	MUC	20	XRF; shipboard
GeoB 8509-2	19°27.03'	18°05.34'	2585	Intrachannel	GC	904	XRF; shipboard
Reference cores							
GeoB 7919-5	20°56.41'	19°23.38'	3420	–	GC	1458	XRF; land-based total carbonate, oxygen isotope data ^a biogenic carbonate, radiocarbon data ^b
CD 53-30	19°42.78'	20°42.81'	3565	–			
ODP 658C	20°45'	18°35'	2263	–			

MUC, multicorer; GC, gravity corer.

^a Extracted from Matthewson et al. (1995).

^b Extracted from deMenocal et al. (2000).

GeoB 8506, GeoB 8507 and GeoB 8509 are under the marginal influence of the organic carbon-rich Cape Blanc depocenter (Bertrand et al., 1996; Martinez et al., 1999). The highly turbiditic core GeoB 8509-2 was recovered from the interior of

the Cap Timiris Canyon directly opposite site GeoB 8507, where the channel widens into a NE-SW elongated basin of about 4 km width and 160 m depth relative to the levees. Incised into this basin is a 200–300 m wide gully or thalweg

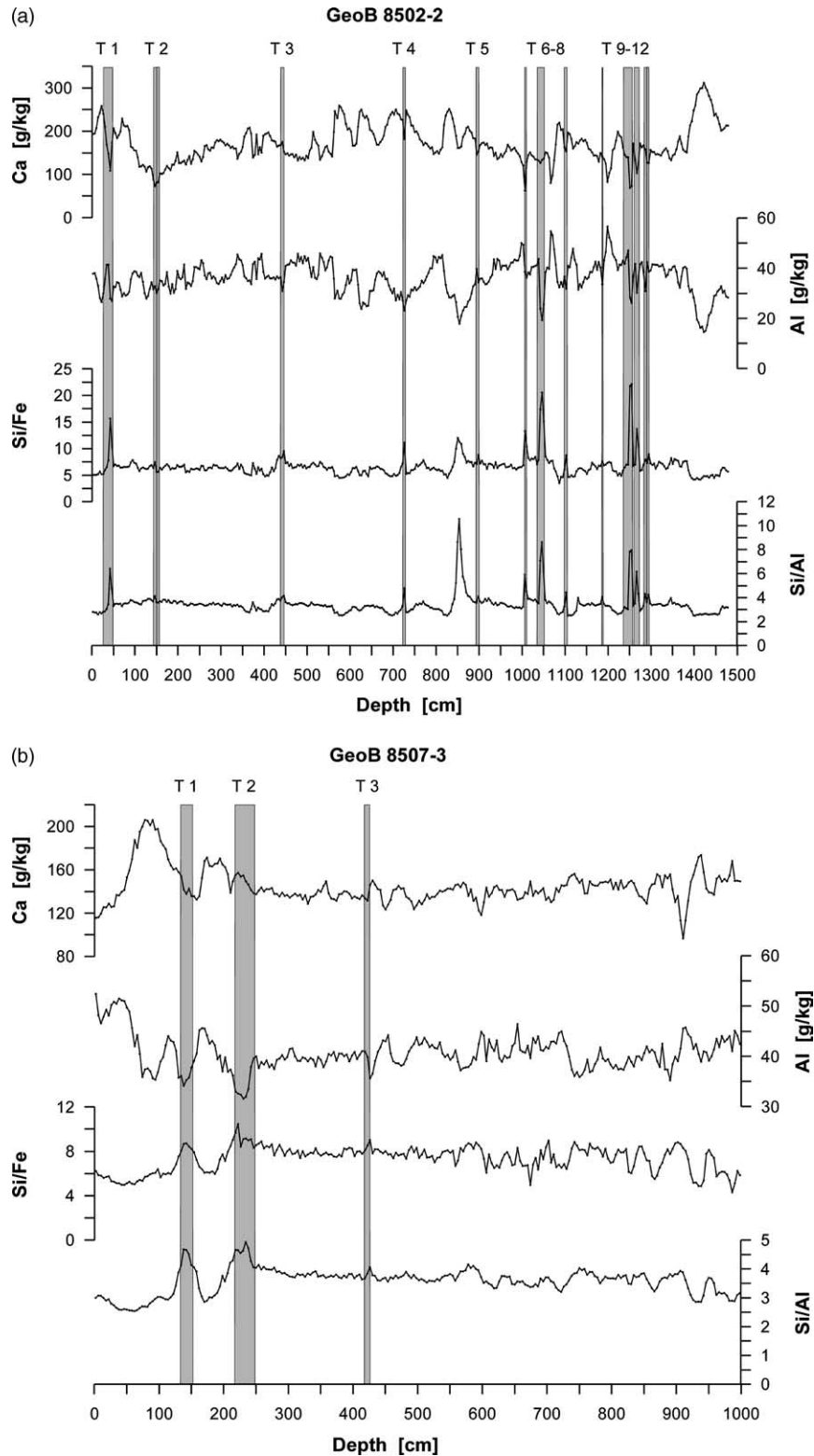


Fig. 2. 2a–d. Ca, Al, Si/Fe and Si/Al downcore profiles in gravity cores from the Cap Timiris Canyon. Grey bars mark the positions of the turbidites. Turbidites have been coded by numbers with T 1 being the most recent. Closed circles in Fig. 2d indicate the depths selected for AMS ^{14}C analyses in core GeoB 8509-2 (see Holz, 2005).

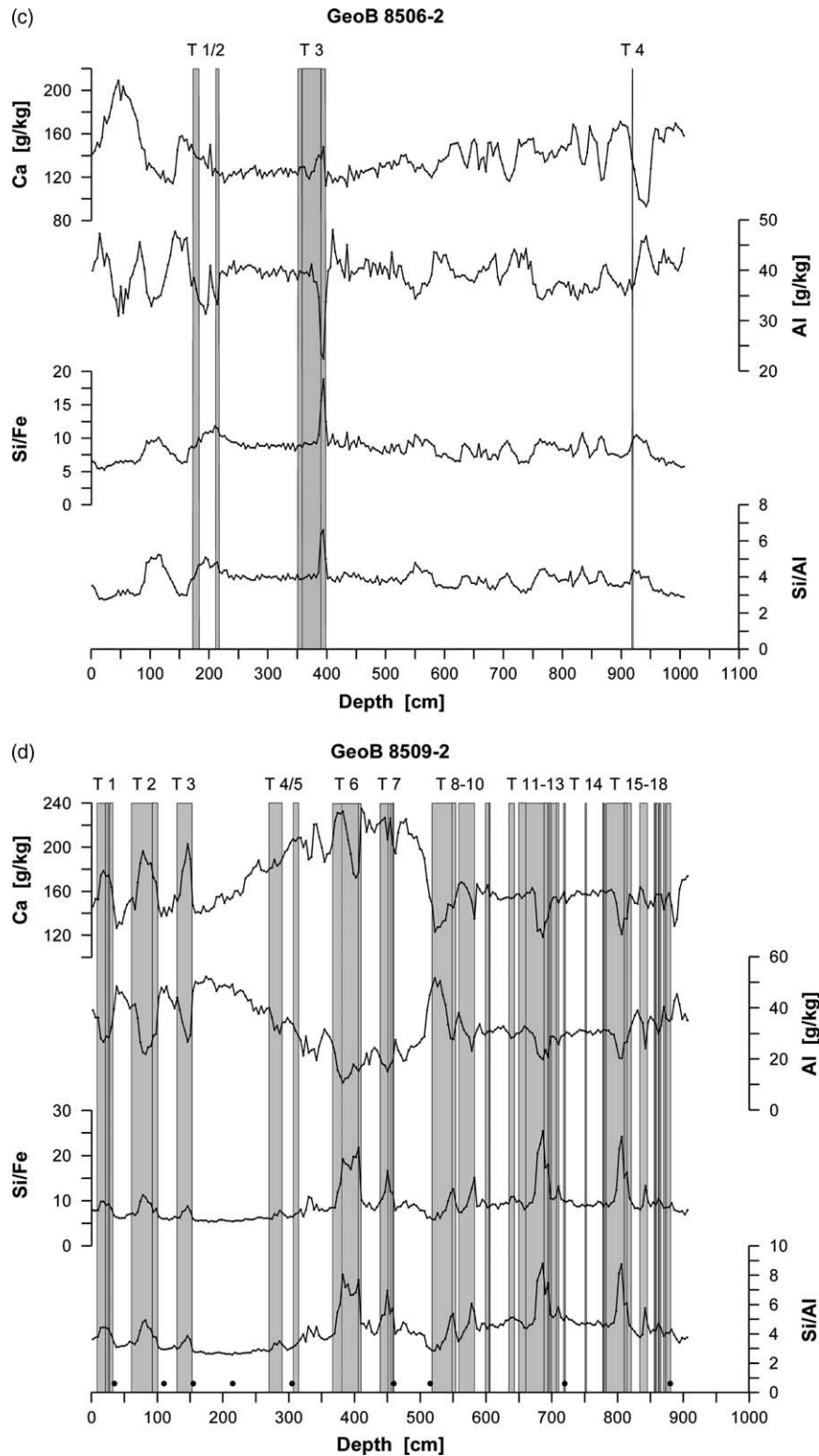


Fig. 2 (continued)

which marks the most active part of the channel (Schulz and Cruise Participants, 2003). It is likely that on exiting the narrow channelised pathway and entering this basin, turbidity currents will lose flow energy, leading to deposition of part of their sediment load. The coarser fraction will settle out of

suspension and will be deposited without major erosion of the substrate. This area with sediment accumulation was sampled to ensure intercalation of turbiditic material with pelagic sediments. A detailed bathymetric map of the Cap Timiris Canyon is published in Krastel et al. (2004).

Gravity core GeoB 7919-5, obtained off Cape Blanc during RV Meteor cruise M 53-1c in April/May 2002 (Meggers and Cruise Participants, 2003), was analysed geochemically prior to our cruise in order to provide a master record for use onboard. Its downcore Ca profile was correlated with detailed total carbonate data of core CD 53-30, retrieved from the Cape Verde Terrace, and well-dated back to ≈ 290 kyr based on Foraminifera $\delta^{18}\text{O}$ records (Matthewson et al., 1995). Core from Ocean Drilling Program (ODP) Site 658C, recovered off Cape Blanc during Leg 108 (Ruddiman et al., 1988), also served as a high resolution reference by supplying a radiocarbon age back to ≈ 25 kyr and detailed biogenic carbonate data (deMenocal et al., 2000; Fig. 1 and Table 1).

4. Methods

4.1. Land-based and onboard geochemical analyses

Downcore element profiles were determined for the reference core GeoB 7919-5 prior to the cruise at Bremen University on syringe samples in 5 cm intervals. The four gravity cores and their corresponding MUCs from the Cap Timiris Canyon were analysed onboard ship. MUCs were sampled at a resolution of 1 cm for the upper 10 cm and a resolution of 2 cm below this depth. Continuous strips of sediment were collected from the gravity cores in plastic U-channels with a cross-section of 1.5×2 cm and the complete U-channel was sectioned in 4 cm increments. All samples were oven-dried at 200 °C for 60 min and ground manually. Reliable contents for eighteen elements (Si, Ti, Al, Fe, Mn, Mg, Ca, K, Sr, Ba, Rb, Cu, Ni, Zn, P, S, Cl and Br) were determined by energy-dispersive polarisation X-ray fluorescence (EDPXRF) spectrometry using a Spectro Xepos instrument. Analytical quality was assessed by daily analyses of a pressed pellet of MAG-1 standard reference material (4 g MAG-1 standard powder + 0.9 g Hoechst Wax; e.g. Govindaraju, 1994). The XRF analytical method employed is described in detail elsewhere (Wien et al., 2005). All geochemical data presented in this study are available on the Pangaea database (<http://www.wdc-mare.org/PangaVista?query=@Ref26537>).

4.2. Distinction between turbidites and pelagites

Sediments collected from the Cap Timiris Canyon mainly consist of bioturbated pelagic mud and turbidite layers. Yet a visual distinction between the homogenous upper part of a turbidite and the overlying pelagite is often complicated, especially when there is a gradational transition due to bioturbation instead of a distinct discontinuity at the boundary. A multi-proxy approach was used to determine the limits of the turbidites as exactly as possible. Uncertain bed boundaries were fixed by combined visual investigation of the split core together with corresponding X-ray radiographs, and additional information obtained from grain size (Holz, 2005) and geochemical analyses. Several intercalated turbidites could be clearly distinguished from pelagites by their Si/Al or Si/Fe ratios (Fig. 2a–d). Possible occurrence of depositional

lamination is commonly obscured by intense bioturbation especially if turbidites are thin (Weaver et al., 1992). Lamination is a certain indicator for turbidite deposits whereas uniformly distributed foraminifera within a sediment interval are an indicator of pelagic sediments.

Prior to geochemical correlation of the sediment cores it was necessary to remove from the dataset all analyses made on turbiditic material. Turbidite boundaries from visual sedimentological investigations (core description; X-ray radiographs) were read off with 0.5 cm accuracy whereas geochemical analyses were done in 4 cm increments. All XRF samples were taken continuously and therefore, sample breaks did not necessarily correspond exactly with observed boundaries between turbidite and pelagite beds. Whenever XRF was performed on a sample containing both sediment types (turbidite/pelagite), it remained within the dataset only if the amount of turbidite material comprised less than half the sample (<2 cm). The resulting error had no direct influence on the correlation as it only affects the analyses immediately above and below the individual turbidite layers and not the pelagic sequences in between. Only sediments which had been unambiguously identified as turbidites were removed from the dataset whereas material which had neither clear pelagic nor turbiditic signature remained. Consequently, the reported amount of turbidite material is the minimum present.

4.3. Core-to-core correlation

The cores from the Cap Timiris Canyon were tied into a stratigraphic framework by correlating their downcore Ca content profiles with carbonate data from the reference cores CD 53-30 (Matthewson et al., 1995) and ODP 658C (deMenocal et al., 2000). Core GeoB 7919-5 was also included as its geochemical data allowed fit of age models for all analysed elements. Since this core was examined pre-cruise using XRF, its whole element suite supplemented carbonate data of the two reference cores. Prior to correlation, MUCs were tied to the tops of their corresponding gravity cores as the core tops of the latter were disturbed by the coring process. The overlapping section was determined on the absolute values of the major elements. The geochemical analyses of the top few centimetres of the gravity core were substituted by the equivalent higher resolution analyses of the MUC. The MUC tops are defined to have an age of 0 kyr, representing the present sediment surface.

Correlation and fitting of ages to the pelagic intervals of all cores were made by linear interpolation between tie points using the software 'AnalySeries', version 1.1 (Paillard et al., 1996). Each turbidite was numbered according to its position within the sedimentary sequence, with T 1 at the top (most recent) and T X at the base. In the following text turbidites will be referred to according to the notation T X-GeoB 85XX. Composite beds where two or more turbidites are deposited directly on top of each other without interbedded pelagites (e.g. T 3-GeoB 8506 in Fig. 2c; T 12-GeoB 8509 in Fig. 2d) are labelled using one number only as it was not possible to decide whether such multiple turbidites were deposited consecutively

in the course of one event or during several subsequent events. Therefore, the labels neither reflect the actual number of turbidite events nor the actual number of turbidite layers. The geochemical age model for core GeoB 8509-2 was constrained using nine accelerator mass spectrometer (AMS) radiocarbon dates of monospecific samples of the planktonic foraminifer *Globigerinoides ruber* (Holz, 2005).

Before applying the correlation technique it was necessary to make some assumptions and to assess possible sources of errors. It was assumed that in the study area pelagites and turbidites were and are still accumulating, and that turbidites caused little or nil erosion. Possible sources of error include uncertainties in precisely defining turbidite-pelagite boundaries, and unidentified turbidites (especially thin mud turbidites). Because of these uncertainties care must be taken with correlation of turbiditic cores.

5. Results

5.1. Geochemical analyses

Turbidite position and selected geochemical data for each core from the Cap Timiris Canyon were plotted to assess downcore variations (Fig. 2a–d). There is a clear contrast between the pelagite and turbidite distribution on the levees and at the intrachannel site. The three levee cores GeoB 8502-2, GeoB 8507-3 and GeoB 8506-2 contain relatively little turbidite sediment ($\approx 6\text{--}8\%$ of the sediment column). Core GeoB 8509-2 taken from the interior of the canyon comprises approximately 42% turbidite material (Table 4). The downcore Ca and Al profiles represent compositional variations in the time-series record and, in addition, indicate a frequent element enrichment or depletion in turbidite layers compared to the over- and underlying pelagites. The element ratios Si/Fe and

Si/Al in contrast represent the amount of siliciclastic material in the turbidites with respect to the pelagic sediments. Note that turbidite layers are often, though not necessarily, characterised by element contents or element ratios which deviate from the general trend. This is best seen in turbidites T 1–3-GeoB 8509 and T 1, 7, 10, 11-GeoB 8502. Occasionally, Si/Fe and Si/Al ratios pretend the presence of turbidites but this may result from sand-filled burrows which can be distinguished from turbidites by core description and X-ray radiographs (e.g. Si/Al and Si/Fe peaks at 850–870 cm depth in GeoB 8502-2, at ≈ 110 cm depth in GeoB 8506-2).

5.2. Age models for the pelagites

An age model was initially fitted from the $\delta^{18}\text{O}$ dated reference core CD 53-30 (Matthewson et al., 1995) via GeoB 7919-5 to GeoB 8502-2 by correlation of total carbonate and downcore Ca variation (Fig. 3). All three cores extend from the present to nearly 290 kyr. The geochemical data suggest a hiatus is present in the lower part of GeoB 8502-2 (indicated by a question mark in Fig. 3). This hiatus comprises nearly the entire OIS 7 and occurs at the same stratigraphic position where a hiatus of approximately 37 kyr is recorded in core CD 53-30. The latter is probably due to an erosive event which deposited a thin turbidite layer (Matthewson et al., 1995). However, no mass gravity deposit is seen in core GeoB 8502-2.

The Ca record of the pelagites from the intrachannel core GeoB 8509-2 was correlated with ODP Core 658C, taking advantage of its detailed biogenic carbonate record for the last 25 kyr (deMenocal et al., 2000; Fig. 4). Note that only the last 14.8 kyr of ODP 658C carbonate data are shown in Fig. 4 as there is a hiatus between 14.8 and 17.4 kyr. According to the correlation, GeoB 8509-2 dates back to ≈ 15 kyr. This age model agrees with the radiocarbon data (Holz, 2005) for the

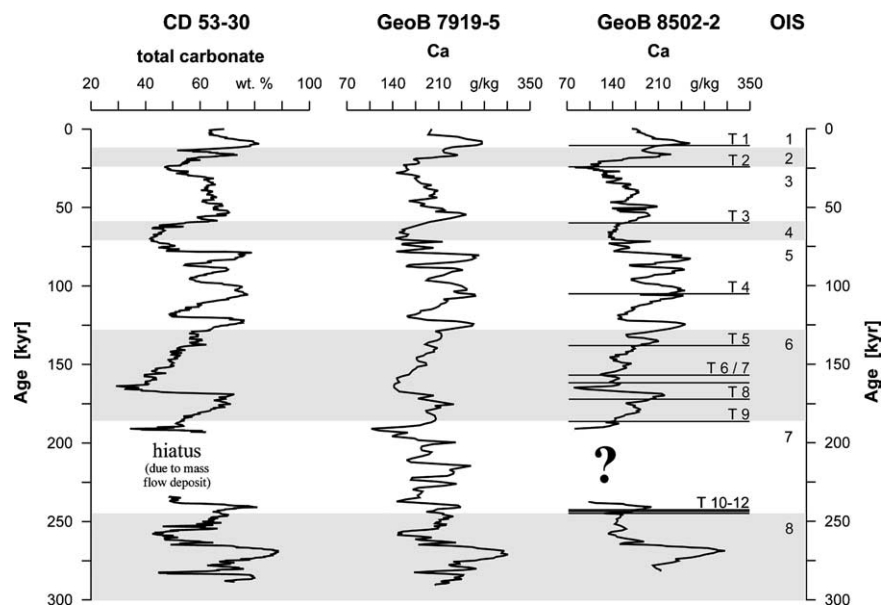


Fig. 3. Correlation of the cores CD 53-30 (Matthewson et al., 1995), GeoB 7919-5 and GeoB 8502-2 based on total carbonate and Ca data. T 1 to T 10 mark the downcore positions of turbidites present in core GeoB 8502-2. The question mark indicates the interval where part of the sediment in this core is presumed to be missing. A hiatus at the same stratigraphic position in reference core CD 53-30 is due to erosion by a mass gravity flow.

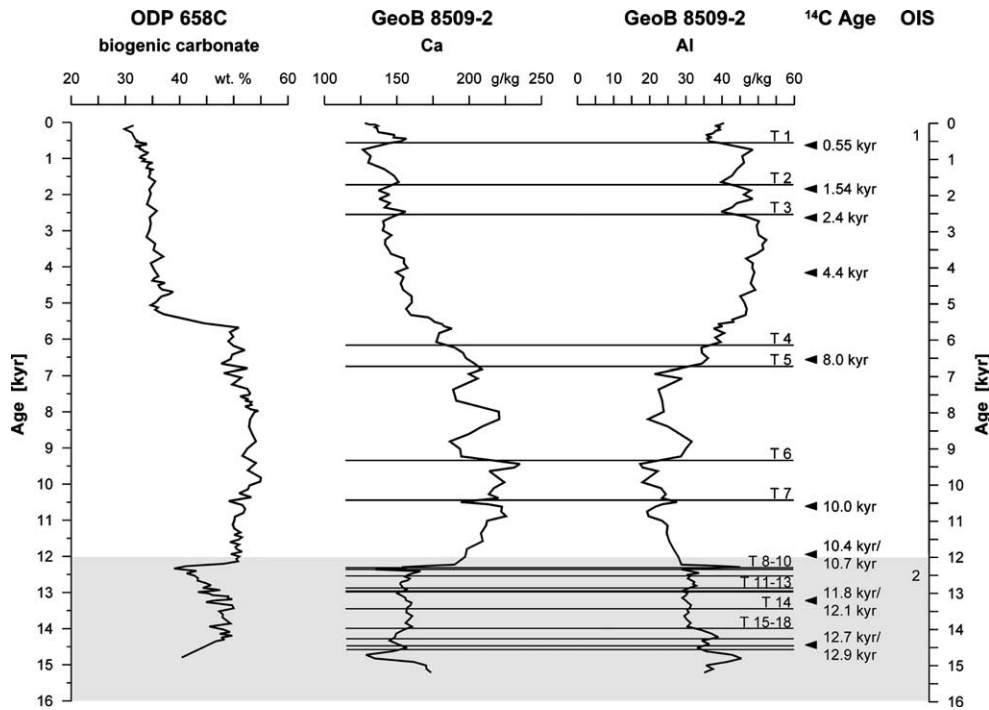


Fig. 4. Correlation of GeoB 8509-2 Ca data with biogenic carbonate data for the upper 3.3 m (the last 14.8 kyr) of the reference core from ODP Site 658C (deMenocal et al., 2000). Also shown is the Al record of GeoB 8509-2 which mirrors the Ca content profile. The positions of the AMS ¹⁴C analyses in core GeoB 8509-2 are indicated by arrows. These ages agree for the last 5 kyr, however, discrepancies can be observed at older time. AMS ¹⁴C data from Holz (2005).

last 5 kyr, however, discrepancies of up to 1.9 kyr between the radiocarbon data and the fitted age model are seen in the lower part of the core. Four radiocarbon ages are younger than would be predicted by the correlation and one is older (Table 2).

The cores GeoB 8506-2 and GeoB 8507-3 were adjusted using their Ca and Al data (Figs. 5 and 6), and fitted with age models by correlation with GeoB 8502-2. This correlation is reliable for the upper two distinct Ca peaks in cores GeoB 8506-2 and GeoB 8507-3 which date back to ≈ 20 kyr. Below these peaks, correlation up to ≈ 55 kyr was more difficult as the Ca content profiles lack significant peaks. Lastly, Ca profiles from all cores from the Cap Timiris Canyon were plotted as shown in Fig. 6.

5.3. Turbidite emplacement times

As can be seen in Figs. 3 and 6, turbidity currents delivered sediments predominantly at stage boundaries and during glacial periods. Turbidites at the levee sites GeoB 8502, GeoB 8507 and GeoB 8506 were emplaced at transitions from

Table 2
Discrepancies between radiocarbon data and fitted age model at five depths in core GeoB 8509-2

Depth (cm)	Radiocarbon age (kyr)	Geochemical age model (kyr)	Discrepancy (kyr)
305	8.0	6.7	1.3
460	10.0	10.4	0.4
515	10.4/10.7	12.2	1.8/1.5
720	11.8/12.1	13.0	1.2/0.9
881	12.7/12.9	14.3	1.6/1.4

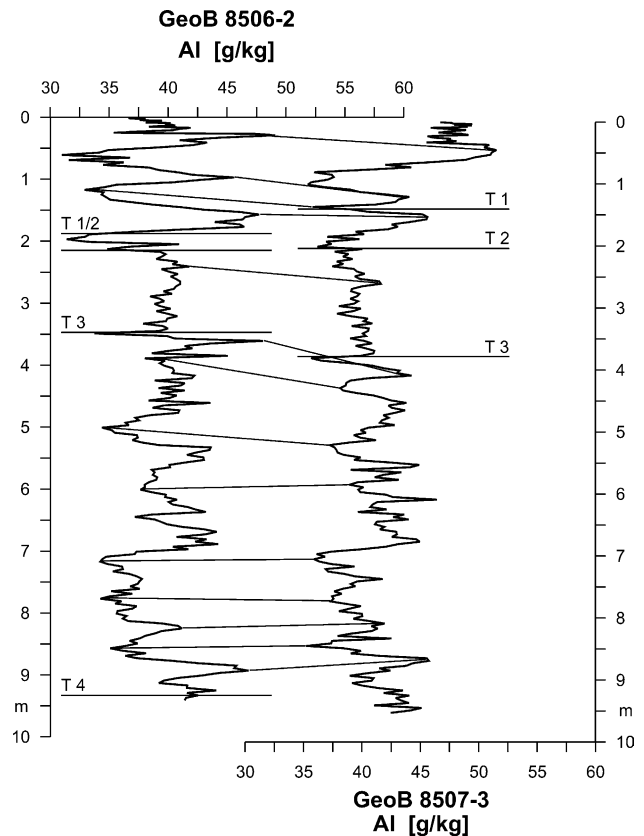


Fig. 5. Correlation of downcore Al data on the cores GeoB 8506-2 and GeoB 8507-3.

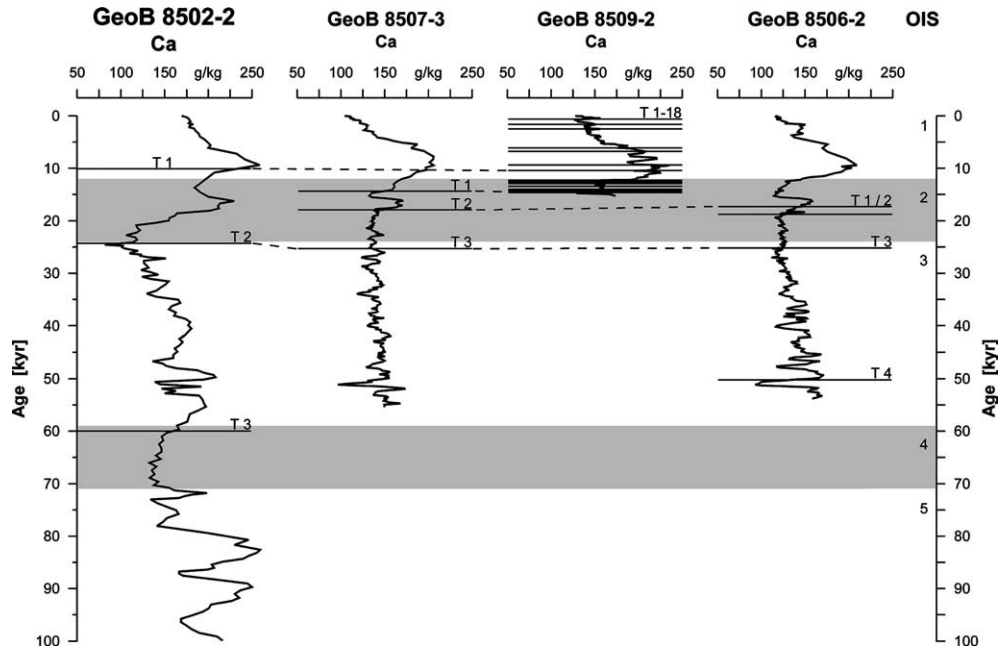


Fig. 6. Age models for the four cores GeoB 8502-2, GeoB 8507-3, GeoB 8509-2 and GeoB 8506-2 from the Cap Timiris Canyon based on correlation of their downcore Ca content profiles. Dotted lines indicate well-correlated turbidite layers. The entire length of core GeoB 8502-2 is not shown but for illustration purposes only the interval back to an age of 100 kyr.

glacial to interglacial/interstadial, and at transitions from interglacial/interstadial to glacial. Eight turbidites are at mid-stage positions during glacial OISs 6 and 2. Only T 4-GeoB 8502 and T 4-GeoB 8506 were deposited during interglacial OIS 5 and interstadial OIS 3, respectively.

A clear contrast can be seen at intrachannel site GeoB 8509 where most turbidites (T 18-8-GeoB 8509) are linked to late glacial OIS 2 and the stage boundary 1/2 whereas the remainder (T 7-1-GeoB 8509) was deposited during Holocene time (OIS 1). The three most recent turbidites at this site were emplaced ≈ 0.5 , 1.7 and 2.5 kyr ago. Owing to the very different ages and thus, sedimentation rates of the four study cores, it was rarely possible to link intrachannel turbidites and overspill turbidites on the levees across the Cap Timiris Canyon. Only four examples where two or three deposits may be related to the same turbidite event were recognised at ≈ 10 , at ≈ 14 , at 17–18 and at 24–25 kyr (Fig. 6 and Table 3).

5.4. Pelagic and turbidite sedimentation rates

Average sedimentation rates were determined from these age models for the pelagic and intercalated turbidite beds of all study cores (Table 4). Note that in this study all sedimentation rates have been calculated over the entire core lengths and not back to a certain age, owing to the very different time-resolutions of the cores. For the three levee sites, pelagic sedimentation rates vary significantly, being lowest (≈ 7.0 cm/kyr) at the deepest site GeoB 8502 and increasing significantly upslope nearly three-fold to 17–18 cm/kyr at sites GeoB 8507 and GeoB 8506. The most prominent shift, however, occurs at the intrachannel site GeoB 8509

(≈ 35 cm/kyr) where pelagic sedimentation rates are doubled compared to the directly adjacent levee site GeoB 8507.

Turbidite sedimentation rates are low (between ≈ 0.7 and 1.2 cm/kyr) at the levee locations, but show much higher average values of ≈ 25 cm/kyr at the intrachannel site. Owing to the temporally very different turbidite abundances at the latter location, sedimentation rates were calculated separately for the Holocene (0–12 kyr) and the late Pleistocene (12–15.2 kyr). The values indicate that the pre-Holocene turbidites at the intrachannel site had accumulated at an average rate of approximately 64 cm/kyr with an average recurrence interval of ≈ 300 years. In contrast, average sedimentation rates for Holocene turbidites are much lower (≈ 15 cm/kyr) with a recurrence interval of ≈ 1.7 kyr in average (Fig. 4).

Core GeoB 8509-2 from the interior part of the Cap Timiris Canyon shows a change in sediment geochemistry between ≈ 5.2 and ≈ 3.0 m depth which corresponds to the age between ≈ 12.3 and ≈ 6.5 kyr. This change is clearly visible in the Ca and Al content profiles (Figs. 2d and 4) where Ca shows a shift to higher and Al a depletion to lower values between 5.2 and 3.0 m.

6. Discussion

6.1. Turbidite emplacement in the Cap Timiris Canyon

Indirect dating has allowed ages of emplacement to be assigned to each turbidite unit and thus allows estimation of the frequency of turbidite emplacement in the Cap Timiris Canyon. Turbidites in the lower part of core GeoB 8502-2 suggest that the Cap Timiris Canyon was active for at least the last 245 kyr. On this time scale, the data, especially on the three levee cores, suggest turbidite activity was controlled by

Table 3
Core number, location in the canyon system, turbidite notation, turbidite depth and turbidite emplacement time in all study cores from the Cap Timiris Canyon as determined from the geochemical age models

Core no.	Location in canyon system	Turbidite no.	Turbidite depth (cm)	Turbidite emplacement time (kyr)	
GeoB 8502-2	Levee	T 1	25–47	10.1	
		T 2	142–155	24	
		T 3	437.5–445	60	
		T 4	722–727	105	
		T 5	892–898	138	
		T 6	1005–1009	157	
		T 7	1034–1050	162	
		T 8	1096.5–1103	172	
		T 9	1184.5–1186.5	188	
		T 10	1234.5–1254.5	243	
		T 11	1259–1271	243	
		T 12	1282–1293	245	
GeoB 8506-2	Levee	T 1	172–182	17.3	
		T 2	211–216	18.9	
		T 3	350–397	25	
		T 4	918–919	50	
GeoB 8507-3	Levee	T 1	133–151	14.4	
		T 2	217–247	17.9	
		T 3	417–425	25	
GeoB 8509-2	Intrachannel	T 1	8–32	0.5	
		T 2	60–100	1.7	
		T 3	129–152.5	2.5	
		T 4	269–289	6.1	
		T 5	306–314	6.7	
		T 6	366–409	9.3	
		T 7	438–459	10.4	
		T 8	517–553	12.3	
		T 9	557.5–581.5	12.3	
		T 10	598–605	12.5	
		T 11	634–642	12.9	
		T 12	649–710	12.9	
		T 13	717–719.5	13.0	
		T 14	750–752	13.4	
		T 15	777–780.5	14.0	
				782–820	
				833–844.5	14.3
				855–856.5	14.5
		857.5–861.5			
		862.5–865			
		868.5–871.5	14.6		
		873.5–880			

Table 4
Core number, location in the canyon system, percent of sediment column made up of turbidites, maximum ages and average pelagic and turbiditic sedimentation rates

Core no.	Location in canyon system	Percent of sediment column made up of turbidites (%)	Maximum age at base of core (kyr)	Average pelagic sedimentation rates (cm/kyr)	Average turbidite sedimentation rates (cm/kyr)
CD 53-30	–	–	≈ 290	2.4; variation between 1.5 and 5.6	–
GeoB 7919-5	–	–	≈ 290	4.6	–
ODP 658C	–	–	≈ 25	18	–
GeoB 8502-2	Levee	8	≈ 190 ^a (?280 ^b)	7.0 ^a	0.7 ^a
GeoB 8507-3	Levee	6	≈ 55	17	1.0
GeoB 8506-2	Levee	6	≈ 55	18	1.2
GeoB 8509-2	Intrachannel	42	≈ 15	35 (28 ^c ; 63 ^d)	25 (15 ^c ; 64 ^d)

Sedimentation rates were calculated from the maximum age at the base of each core instead of a corresponding age for all cores. Average pelagic sedimentation rates for core CD 53-30 are from Matthewson et al. (1995); for core ODP 658C from deMenocal et al. (2000).

^a At ≈ 12 m core length.

^b At ≈ 14.8 m core length.

^c From 0 to 12 kyr.

^d From 12 to 15.2 kyr.

sea-level fluctuations over the last glacial-interglacial cycles. Turbidity currents seem to have been preferentially triggered at stage boundaries at changes from one climatic regime to another, accompanied both by sea-level changes (cf. Weaver and Kuijpers, 1983; Weaver and Rothwell, 1987; Simm et al., 1991; Rothwell et al., 1992; Weaver et al., 1992; Lopez, 2001; Wynn et al., 2002) and perhaps changes in the ocean current system during sea-level low-stands (cf. Shanmugam and Moiola, 1982; 1984; Stow et al., 1984; Posamentier and Vail, 1988; Lopez, 2001).

The most detailed record of turbidity current activity at the transition from the last glacial to the Holocene is preserved in the intrachannel core GeoB 8509-2. The Ca record of this core corresponds to the carbonate record of the reference core from ODP Site 658C where shifts in sediment composition indicate the onset and termination of the African Humid Period (14.8 and 5.5 kyr) and the termination of the Younger Dryas cool period (12.3 kyr; deMenocal et al., 2000). Turbidites at site GeoB 8509 clearly accumulated during the end of the last glacial period and occur with an average emplacement frequency of 1 event every 300 years from the beginning of the African Humid Period until the end of the Younger Dryas cool period. These events occurred during the deglaciation and the rapid sea-level rise at the Pleistocene/Holocene transition. Turbidity current activity in the Cap Timiris Canyon decreases, but does not cease, during the Holocene and therefore, provides an example for continued mass transport at a time of high sea-level, as has also been noted in other turbidite settings (e.g. Weber et al., 1997; 2003; Babonneau et al., 2002; Wynn et al., 2002; Droz et al., 2003).

The correlation of core GeoB 8509-2 with ODP Site 658C highlights a discrepancy between the geochemical age model and the radiocarbon ages especially in the lower half of the core. The higher radiocarbon age of 7.95 kyr (geochemical age model: 6.7 kyr) may possibly be explained by supply of older material from the upper slope through a turbidite event. This explanation, however, cannot be applied to the radiocarbon ages which are younger than predicted by the correlation. However, for the purpose of correlation the ODP 658C carbonate data were the most appropriate choice because this site is located close to the Cap Timiris Canyon at a similar water depth as GeoB 8509. The high resolution carbonate profile of this reference core for the last 25 kyr allowed the best fit of an age model to our study core GeoB 8509-2.

Turbidity current activity in the Cap Timiris Canyon often coincides with other reported mass transport events along the NW African continental margin and in the Mediterranean Sea (Table 5). Deposition of turbidite T 2-GeoB 8502 at 24 kyr, for example, corresponds to the emplacement of the Balearic Basin Megaturbidite in the Western Mediterranean Sea around 22 kyr at the height of the last glacial maximum (Rothwell et al., 2000). At this time, sea-level approached its lowest stand during the last 130 kyr, approximately 120 m relative to the present (Shackleton, 1987). Turbidite T 3-GeoB 8502 (60 kyr) occurs at approximately the same time as the Saharan Debris Flow (60 kyr; Gee et al., 1999) and turbidites *d* on the Madeira Abyssal Plain (Rothwell et al., 1992; Weaver et al., 1992), *AB5*

in the Agadir Basin (Wynn et al., 2002) and *Se* on the Seine Abyssal Plain (Davies et al., 1997) which were emplaced 59 kyr ago at the stage boundary 3/4. Deposition of turbidite T 8-GeoB 8502 at 172 kyr is almost synchronous with a ≈ 170 kyr old slide that onlaps a distal part of the canyon (Krastel et al., 2004). However, apparent synchronous emplacement of turbidites in the Cap Timiris Canyon with mass flow deposits from different source areas suggests temporal episodes of instability and deposition of separate events closely spaced in time. Mass flow deposits from other regions do not correlate with the turbidites in the Cap Timiris Canyon.

6.2. Sea-level control on turbidite emplacement

Sea-level changes seem to be important driving forces for the advective sediment flux through a canyon. Our data support findings in this regard, and even though they do not furnish information on the underlying physical mechanisms, which are to date still poorly understood, we may speculate about these mechanisms. Relative sea-level changes control the accommodation space available for sediments (e.g. Posamentier et al., 1988; Posamentier and Vail, 1988; Vail et al., 1991), and within this context, several factors may possibly govern the stability of the accumulated sediment masses on a passive continental margin. Sea-level fall, for one, causes enhanced sediment transport to the shelf edge, thereby inducing depositional oversteepening of the slope. Once the sea-level falls below the shelf break a loss of buoyancy in the upper slope sediments may promote slope instability. Sea-level changes also influence the hydrostatic pressure on a sediment column. Excess pore water pressure in the near-surface sediments may, for example, result from low permeability of overlying sediments and/or high sedimentation rates (e.g. Einsele et al., 1996). In addition, sea-level changes may induce changes in the circulation pattern and hydrological properties of the bottom (e.g. contour) currents which can undercut the foot of the slope and erode, mould, transport and redistribute sediments (cf. Simm et al., 1991; Einsele, 1996; Weaver et al., 2000; Imbo et al., 2003). The magnitude of sea-level change has further been suggested to broadly correlate with the volume of turbidites on the Madeira Abyssal Plain (Weaver and Rothwell, 1987).

6.3. Sedimentation rates in the Cap Timiris Canyon

The large range of average pelagic sedimentation rates recorded at the four core sites in the Cap Timiris Canyon reflects their different depositional environments and different response to factors such as terrigenous input, regional productivity, or dynamic settings within the canyon system. All sites receive high eolian input due to their positions below the African dust plume (Tetzlaff and Wolter, 1980; Pye, 1987; Wefer and Fischer, 1993). However, site GeoB 8502 is located in a deeper, more distal part of the canyon well outside the high-productivity upwelling region off Cape Blanc. Consequently, sediments here show less high pelagic sedimentation

Table 5
Compilation of mass gravity flows that coincide with turbidites in the Cap Timiris Canyon

Turbidite no. in GeoB 8502-2	Emplacement time (kyr)	Turbidite no. in GeoB 8506-2	Emplacement time (kyr)	Turbidite no. in GeoB 8507-3	Emplacement time (kyr)	Turbidite no. in GeoB 8509-2	Emplacement time (kyr)	Emplacement synchro- nous with...	Climate/sea-level changes
						T 1	0.5	Turbidite <i>a</i> , MAP (<1 kyr) ^{a,b} Turbidite AB1, AB (<1 kyr) ^c	
						T 2	1.7		
						T 3	2.5		
						T 4	6.1		
						T 5	6.7		
						T 6	9.3		
T 1	10.1					T 7	10.4		
						T 8	12.3	Turbidite <i>b</i> , MAP (12 kyr) ^{d,b} Turbidite AB2, AB (12 kyr) ^c	Stage boundary 1/2 (12 kyr); Termination I;
						T 9	12.3	Turbidite <i>S_c</i> , SAP (12 kyr) ^e	Rapid sea-level rise at Pleistocene/Holocene transition
						T 10	12.5		
						T 11	12.9	Mauritanian Slide Complex (≈ 11 – 14 kyr; own unpublished data)	
						T 12	12.9		
						T 13	13.0		
						T 14	13.4		
						T 15	14.0		
				T 1	14.4	T 16	14.3	Canary Debris Flow (15 kyr) ^f	
		T 1	17.3	T 2	17.9	T 17	14.5		Lowest sea-level (-120 m) during Weichselian glaciation ^g
		T 2	18.9			T 18	14.6		
T 2	24	T 3	25	T 3	25			Balearic Basin Mega- turbidite (≈ 22 kyr) ^h	Stage boundary 2/3 (24 kyr); rapid sea-level lowering to its lowest stand (-120 m) during Weichselian glaciation ^g
								Turbidite AB3, AB (24 kyr) ^c Turbidite <i>S_d</i> , SAP (24 kyr) ^e Herodotus Basin Mega- turbidite (≈ 27 kyr) ^{i,h}	
T 3	60	T 4	50					Turbidite <i>d</i> , MAP (59 kyr) ^{d,a}	Stage boundary 3/4 (59 kyr)

		Turbidite AB5, AB (59 kyr) ^c Turbidite Se, SAP (59 kyr) ^c Saharan Debris Flow (60 kyr) ^j	
T 4	105	Turbidite Sh, SAP (≈ 100 kyr) ^c	
T 5	138	Turbidite AB13, AB (130–190 kyr) ^c	Rapid sea-level lowering to its lowest stand (–150 m) during Saalian glaciation ^k
T 6	157	Turbidite Si, Sj, Sk, Sl, SAP (130–150 kyr) ^c Cape Blanc Debris Flow (155 kyr; own unpublished data)	
T 7	162		
T 8	172	Major sediment slide onlapping the levees of the distal Cap Timiris Canyon (170 kyr) ^l	
T 9	188	Turbidites <i>g</i> and <i>g</i> ₁ , MAP (186 kyr) ^{d,a} Turbidite AB14, AB (190 kyr) ^c Turbidite Sr, Ss, SAP (244 kyr) ^c	Stage boundary 6/7 (186 kyr)
T 10	243	Turbidite <i>i</i> , MAP (245 kyr) ^{d,a}	Stage boundary 7/8 (245 kyr); Termination III
T 11	243	Turbidite Sr, Ss, SAP (244 kyr) ^c	
T 12	245		

Synchronous units may have been triggered at the same sea-level/climatic conditions but they are not correlative with the turbidites in the Cap Timiris Canyon. AB, Agadir Basin; MAP, Madeira Abyssal Plain; SAP, Seine Abyssal Plain; LGM, Last Glacial Maximum.

^a Weaver et al. (1992).

^b Weaver and Thomson (1993).

^c Wynn et al. (2002).

^d Rothwell et al. (1992).

^e Davies et al. (1997).

^f Masson (1996).

^g Shackleton (1987).

^h Rothwell et al. (2000).

ⁱ Reeder et al. (2000).

^j Gee et al. (1999).

^k Chappell and Shackleton (1986).

^l Krastel et al. (2004).

rates of ≈ 7.0 cm/kyr which are similar to values of ≈ 4.6 cm/kyr in core GeoB 7919-5 and ≈ 1.5 – 5.6 cm/kyr in core CD 53-30 (Matthewson et al., 1995).

Higher sedimentation rates are seen at the levee sites GeoB 8506 and GeoB 8507. Both sites are positioned in the more proximal part of the canyon and receive higher aeolian input from the African dust plume. Additionally, they are under the marginal influence of the upper slope Cape Blanc depocenter which today extends northwards from approximately 20° to 22° N between 1000 and 2000 m water depth (Fütterer, 1983; Bertrand et al., 1996; Martinez et al., 1999). For ODP Site 658C, which is located $\approx 1^\circ$ further to the north off Cape Blanc at a water depth of 2263 m, an average sedimentation rate of ≈ 18 cm/kyr is reported by deMenocal et al. (2000). This value agrees with our findings for sites GeoB 8506 and GeoB 8507. According to our age model, average pelagic sedimentation rates appear to be doubled at site GeoB 8509 with respect to the directly adjacent levee structure (site GeoB 8507). These high sedimentation rates at site GeoB 8509 provide a detailed temporal resolution for determining turbidite emplacement times.

High productivity off Cape Blanc and the African dust plume principally account for the increased average pelagic sedimentation rates at the levee sites in the canyon system. High sedimentation may also be attributed to turbidite overspill which results from separation from a turbidite flow during downslope transport. The sandy bedload is restricted to the canyon pathway whereas the fine grained suspended fraction may be unconfined and can overspill onto the adjacent levee structures (Masson, 1994; Wynn et al., 2002). This laterally dispersed mud on the levees cannot always be identified conclusively as individual turbidites (Dott, 1983; Einsele et al., 1996). It may dilute pelagites without actually forming distinct layers and thus is reflected in enhanced pelagic sedimentation rates. This dilution effect may also be the reason for the remarkably low amount of identifiable turbidite material at levee site GeoB 8507 ($\approx 6\%$) in contrast to the directly adjacent highly turbiditic site GeoB 8509 ($\approx 42\%$).

6.4. Erosiveness of turbidites

Significant intra-element correlations are seen between total carbonate and the Ca data of cores CD 53-30 (Matthewson et al., 1995), GeoB 7919-5 and the turbidite-bearing levee core GeoB 8502-2. Despite interbedded turbidites, the latter core does not show significant omission of pelagic material except for one sediment sequence in the lower part. We suggest this hiatus results from the same erosive event which deposited the thin turbidite layer in core CD 53-30 (Matthewson et al., 1995). Most likely this event was triggered at the time of sea-level lowering at the stage boundary 6/7 around 190 kyr (cf. Fig. 3).

It is unlikely that even larger-volume turbidity currents travelling channelised in the Cap Timiris Canyon eroded more than a few centimetres into the underlying substrate at the distal levee site GeoB 8502. The good correspondence with the reference cores supports virtually non- or minor-erosive turbidity currents at the low gradient slope off NW Africa (e.g.

Weaver and Kuijpers, 1983; Masson, 1994; Weaver, 1994). This seems also to be true for the two other levee-cores GeoB 8506-2 and GeoB 8507-3 further upslope.

Even at intrachannel site GeoB 8509 sedimentation has been accumulative at least over the last 15 kyr. Groups of turbidite layers are frequently amalgamated to form thicker composite beds such as T 1, 6, 12, 15-GeoB 8509 (cf. Fig. 2d). This suggests that either one series of overlying turbidite layers was fed from several tributaries during the same event or in several, consecutive phases. Alternatively, originally subjacent pelagites may have been eroded and entrained into the turbidite flow during the next event (Weaver, 1994).

The young canyon fill at intrachannel site GeoB 8509 raises the question of how long this accumulative state can be maintained. Eventually, persistent high sedimentation rates in this part of the canyon will mean that it will become filled with sediments. Some large-scale turbidite events should be sufficient to clear the pathway, however. Although during the Holocene only small volume turbidites were emplaced, larger-volume turbidites were deposited during other times and apparently were erosive enough to remove the previous canyon fill and thus maintain the pathway (for instance such as those that deposited the distinctive layers on the levees especially during glacial OISs or at stage boundaries). We suggest highly erosive turbidite events at the stage boundary 2/3 (cf. T 2-GeoB 8502, T 3-GeoB 8507 and T 3-GeoB 8506 in Fig. 6) and within glacial OIS 2 around 17–18 kyr (cf. T 1-GeoB 8506 and T 2-GeoB 8507 in Fig. 6).

7. Conclusions

Application of core-to-core correlation to disturbed sedimentary sequences can be a reliable method of specifying ages for mass transport processes and can add to our knowledge of turbidity current processes and their relationship to sea-level/climatic changes. Element data together with appropriately developed age models can be used to:

- (1) estimate the emplacement times of turbidites,
- (2) estimate the frequency of turbidite emplacement with respect to climatic and sea-level changes, and
- (3) provide information to quantify mass transport within canyon systems.

The age models for pelagites and turbidites presented in this study provide data which are necessary to create a mass balance for gravity-driven downslope transport in the Cap Timiris Canyon. Although, of course, seismo-acoustic and sedimentological data are essential to determine the areal and spatial distribution of turbidite deposits and to understand and quantify the processes of turbidity current production.

Acknowledgements

We are indebted to Karsten Enneking, Simone Pannike, Luzie Schnieders and all other cruise participants for assisting with the laboratory work during the RV Meteor cruise M 58-1.

We likewise owe thanks to the Captain and crew members. The quality of the manuscript was improved by helpful suggestions of two anonymous reviewers. This research was supported by a grant from the DFG Research Centre Ocean Margins at Bremen University.

References

- Babonneau, N., Savoye, B., Cremer, M., Klein, B., 2002. Morphology and architecture of the present canyon and channel system of the Zaire deep-sea fan. *Marine and Petroleum Geology* 19 (4), 445–467.
- Bertrand, P., Shimmield, G., Martinez, P., Grousset, F., Jorissen, F., Paterne, M., Pujol, C., Bouloubassi, L., Buat-Ménard, P., Peypouquet, J.-P., Beaufort, L., Sicre, M.-A., Lallier-Vergès, E., Foster, J.M., Ternois, Y., other participants of the Sedorqua program, 1996. The glacial ocean productivity hypothesis: the importance of regional temporal and spatial studies. *Marine Geology* 130 (1–2), 1–9.
- Bouma, A.H., 1962. Sedimentology of Some Flysch Deposits, a Graphic Approach to Facies Interpretation. Elsevier, Amsterdam. 168 pp.
- Bouma, A.H., 2000. Coarse-grained and fine-grained turbidite systems as end member models: applicability and dangers. *Marine and Petroleum Geology* 17 (2), 137–143.
- Bouma, A.H., Normark, W.R., Barnes, N.E., 1985. Submarine Fans and Related Turbidite Systems. Springer, Berlin. 351 pp.
- Chappell, J., Shackleton, N.J., 1986. Oxygen isotopes and sea level. *Nature* 324, 137–140.
- Davies, T.L., Van Niel, B., Kidd, R.B., Weaver, P.P.E., 1997. High-resolution stratigraphy and turbidite processes in the seine abyssal plain, Northwest Africa. *Geo-Marine Letters* 17 (2), 147–153.
- deMenocal, P., Ortiz, J., Guilderson, T., Adkins, J., Sarnthein, M., Baker, L., Yarusinsky, M., 2000. Abrupt onset and termination of the African humid period: rapid climate responses to gradual insolation forcing. *Quaternary Science Reviews* 19 (1–5), 347–361.
- Diester-Haass, L., Chamley, H., 1982. Oligocene and post-oligocene history of sedimentation and climate off Northwest Africa (DSDP site 369). In: von Rad, U., Hinz, K., Sarnthein, M., Seibold, E. (Eds.), *Geology of the Northwest African Continental Margin*. Springer, Berlin, pp. 529–544.
- Dott, R.H., 1983. Episodic sedimentation—how normal is average? How rare is rare? Does it matter? *Journal of Sedimentary Petrology* 53, 5–23.
- Droz, L., Marsset, T., Ondreas, H., Lopez, M., Savoye, B., Spy-Anderson, F.L., 2003. Architecture of an active mud-rich turbidite system: the Zaire Fan (Congo–Angola margin southeast Atlantic): results from ZaiAngo 1 and 2 cruises. *AAPG Bulletin* 87 (7), 1145–1168.
- Einsle, G., 1996. Event deposits: the role of sediment supply and relative sea-level changes—overview. *Sedimentary Geology* 104 (1–4), 11–37.
- Einsle, G., Chough, S.K., Shiki, T., 1996. Depositional events and their records—an introduction. *Sedimentary Geology* 104 (1–4), 1–9.
- Fütterer, D.K., 1983. The modern upwelling record off Northwest Africa. In: Thiede, J., Suess, E. (Eds.), *Coastal Upwelling: Its Sedimentary Record, Part B. Sedimentary Records of Ancient Coastal Upwelling*. Plenum Press, London, pp. 105–121.
- Gee, M.J.R., Masson, D.G., Watts, A.B., Allen, P.A., 1999. The Saharan debris flow: an insight into the mechanics of long runout submarine debris flows. *Sedimentology* 46, 317–335.
- Govindaraju, K., 1994. 1994 compilation of working values and descriptions for 383 geostandards. *Geostandards Newsletter* 18, 1–158.
- Holz, C., 2005. Climate-induced variability of fluvial and aeolian sediment supply and gravity-driven sediment transport off Northwest Africa. PhD Thesis, University of Bremen, 116 pp. http://elib.suub.uni-bremen.de/publications/dissertations/E-Diss1205_Diss_Holz.pdf.
- Imbo, Y., De Batist, M., Canals, M., Prieto, M.J., Baraza, J., 2003. The Gebra Slide: a submarine slide on the Trinity Peninsula margin, Antarctica. *Marine Geology* 193 (3–4), 235–252.
- Krastel, S., Hanebuth, T.J.J., Antobreh, A.A., Henrich, R., Holz, C., Kölling, M., Schulz, H.D., Wien, K., Wynn, R.B., 2004. Cap Timiris Canyon: a newly discovered channel system offshore of Mauritania. *EOS* 85 (42), 417–432.
- Lancaster, N., Kocurek, G., Singhvi, A., Pandey, V., Deynoux, M., Ghienne, J.-F., Lo, K., 2002. Late pleistocene and holocene dune activity and wind regimes in the western sahara desert of Mauritania. *Geology* 30 (11), 991–994.
- Lopez, M., 2001. Architecture and depositional pattern of the Quaternary deep-sea fan of the Amazon. *Marine and Petroleum Geology* 18 (4), 479–486.
- Martinez, P., Bertrand, P., Shimmield, G.B., Cochran, K., Jorissen, F.J., Foster, J., Dignan, M., 1999. Upwelling intensity and ocean productivity changes off Cape Blanc (Northwest Africa) during the last 70,000 years: geochemical and micropalaeontological evidence. *Marine Geology* 158 (1–4), 57–74.
- Masson, D.G., 1994. Late Quaternary turbidity current pathways to the Madeira Abyssal Plain and some constraints on turbidity current mechanisms. *Basin Research* 6, 17–33.
- Masson, D.G., 1996. Catastrophic collapse of the volcanic island of Hierro 15 ka ago and the history of landslides in the Canary Islands. *Geology* 24 (3), 231–234.
- Matthewson, A.P., Shimmield, G.B., Kroon, D., Fallick, A.E., 1995. A 300 kyr high-resolution aridity record of the North African continent. *Paleoceanography* 10 (3), 677–692.
- Meggens, H., Cruise Participants, 2003. Report and preliminary results of Meteor cruise M 53-1, Limassol–Las Palmas–Mindelo, 30.03.-03.05.2002. *Berichte Fachbereich Geowissenschaften Bremen*, No. 214.
- Paillard, D., Labeyrie, L., Yiou, P., 1996. Macintosh program performs time-series analysis. *EOS Transactions AGU* 77, pp. 379.
- Pearce, T.J., Jarvis, I., 1995. High-resolution chemostratigraphy of quaternary distal turbidites: a case study of new methods for the analysis and correlation of barren sequences. In: Dunay, R.E., Hailwood, E.A. (Eds.), *Non-Biostratigraphical Methods of Dating and Correlation*. Geological Society Special Publication No. 89, pp. 107–143.
- Posamentier, H.W., Vail, P.R., 1988. Eustatic controls on clastic deposition (II)—sequence and systems tract models. In: Wilgus, C.K., Hastings, B.S., Kendall, C.G.S.C., Posamentier, H.W., Ross, C.A., van Wagoner, J.C. (Eds.), *Sea-level Changes: An Integrated Approach*. Society of Economic Paleontologists and Mineralogists Special Publication, Tulsa, pp. 125–154.
- Posamentier, H.W., Jervey, M.T., Vail, P.R., 1988. Eustatic controls on clastic deposition (I)—conceptual framework. In: Wilgus, C.K., Hastings, B.S., Kendall, C.G.S.C., Posamentier, H.W., Ross, C.A., van Wagoner, J.C. (Eds.), *Sea-level Changes: An Integrated Approach*. Society of Economic Paleontologists and Mineralogists Special Publication, Tulsa, pp. 109–124.
- Pye, K., 1987. *Aeolian Dust and Dust Deposits*. Academic Press, London. 334 pp.
- Reeder, M.S., Rothwell, R.G., Stow, D.A.V., 2000. Influence of sea level and basin physiography on emplacement of the late Pleistocene Herodotus Basin Megaturbidite, SE Mediterranean Sea. *Marine and Petroleum Geology* 17 (2), 199–218.
- Rothwell, R.G., Pearce, T.J., Weaver, P.P.E., 1992. Late Quaternary evolution of the Madeira Abyssal Plain, Canary Basin, NE Atlantic. *Basin Research* 4, 103–131.
- Rothwell, R.G., Thomson, J., Kahler, G., 1998. Low-sea-level emplacement of a very large Late Pleistocene ‘megaturbidite’ in the western Mediterranean Sea. *Nature* 392, 377–380.
- Rothwell, R.G., Reeder, M.S., Anastasakis, G., Stow, D.A.V., Thomson, J., Kahler, G., 2000. Low sea-level stand emplacement of megaturbidites in the western and eastern Mediterranean Sea. *Sedimentary Geology* 135 (1–4), 75–88.
- Ruddiman, W., Sarnthein, M., Baldauf, J., Shipboard Scientific Party, 1988. Eastern tropical Atlantic. *Proceedings of the ODP, Initial Reports*, 108 (section 1). Ocean Drilling Program, College Station, TX.
- Schulz, H.D., Cruise Participants, 2003. Report and preliminary results of Meteor cruise M 58-1, Dakar–Las Palmas, 15.04.-12.05.2003. *Berichte Fachbereich Geowissenschaften Bremen*, No. 215.
- Shackleton, N.J., 1987. Oxygen isotopes, ice volume and sea level. *Quaternary Science Reviews* 6 (3–4), 183–190.
- Shanmugam, G., Muiola, R.J., 1982. Eustatic control of turbidites and winnowed turbidites. *Geology* 10, 231–235.

- Shanmugam, G., Muiola, R.J., 1984. Eustatic control of calciclastic turbidites. *Marine Geology* 56 (1–4), 273–278.
- Simm, R.W., Weaver, P.P.E., Kidd, R.B., Jones, E.J.W., 1991. Late Quaternary mass movement on the lower continental rise and abyssal plain off Western Sahara. *Sedimentology* 38, 27–40.
- Stow, D.A.V., Shanmugam, G., 1980. Sequence of structures in fine-grained turbidites: comparison of recent deep-sea and ancient flysch sediments. *Sedimentary Geology* 25 (1–2), 23–42.
- Stow, D.A.V., Howell, D.G., Nelson, C.H., 1984. Sedimentary, tectonic and sea-level controls on submarine fans and slope-apron turbidite systems. *Geo-Marine Letters* 3, 57–64.
- Tetzlaff, G., Wolter, K., 1980. Meteorological patterns and the transport of mineral dust from the North African continent. *Paleoecology of Africa* 12, 31–42.
- Vail, P.R., Audemard, F., Bowman, S.A., Eisner, P.N., Perez-Cruz, C., 1991. The stratigraphic signatures of tectonics, eustasy and sedimentology—an overview. In: Einsele, G., Ricken, W., Seilacher, A. (Eds.), *Cycles and Events in Stratigraphy*. Springer, Berlin, pp. 617–659.
- Vörösmarty, C.J., Fekete, B.M., Meybeck, M., Lammers, R.B., 2000. Global systems of rivers: its role in organizing continental land mass and defining land-to-ocean linkages. *Global Biogeochemical Cycles* 14 (2), 599–621.
- Weaver, P.P.E., 1994. Determination of turbidity current erosional characteristics from reworked coccolith assemblages, Canary Basin, North-east Atlantic. *Sedimentology* 41, 1025–1038.
- Weaver, P.P.E., Kuijpers, A., 1983. Climatic control of turbidite deposition on the Madeira Abyssal Plain. *Nature* 306, 360–363.
- Weaver, P.P.E., Rothwell, R.G., 1987. Sedimentation on the Madeira Abyssal Plain over the last 300,000 years. In: Weaver, P.P.E., Thomson, J. (Eds.), *Geology and Geochemistry of Abyssal Plains*. Geological Society of London Special Publication, pp. 71–86.
- Weaver, P.P.E., Thomson, J., 1993. Calculating erosion by deep-sea turbidity currents during initiation and flow. *Nature* 364, 136–138.
- Weaver, P.P.E., Rothwell, R.G., Ebbing, J., Gunn, D., Hunter, P.M., 1992. Correlation, frequency of emplacement and source directions of megaturbidites on the Madeira Abyssal Plain. *Marine Geology* 109 (1–2), 1–20.
- Weaver, P.P.E., Wynn, R.B., Kenyon, N.H., Evans, J., 2000. Continental margin sedimentation, with special reference to the North-east Atlantic margin. *Sedimentology* 47, 239–256.
- Weber, M.E., Wiedicke, M.H., Kudrass, H.R., Hubscher, C., Erlenkeuser, H., 1997. Active growth of the Bengal fan during sea-level rise and highstand. *Geology* 25 (4), 315–318.
- Weber, M.E., Wiedicke-Hombach, M., Kudrass, H.R., Erlenkeuser, H., 2003. Bengal Fan sediment transport activity and response to climate forcing inferred from sediment physical properties. *Sedimentary Geology* 155 (3–4), 361–381.
- Wefer, G., Fischer, G., 1993. Seasonal patterns of vertical particle flux in equatorial and coastal upwelling areas of the Eastern Atlantic. *Deep Sea Research Part I: Oceanographic Research Papers* 40 (8), 1613–1645.
- Wien, K., Wissmann, D., Kölling, M., Schulz, H.D., 2005. Fast application of x-ray fluorescence spectrometry aboard ship: how good is the new portable spectro xepos analyser? *Geo-Marine Letters* 25 (4), 248–264.
- Wynn, R.B., Masson, D.G., Stow, D.A.V., Weaver, P.P.E., 2000a. The Northwest African slope apron: a modern analogue for deep-water systems with complex seafloor topography. *Marine and Petroleum Geology* 17 (2), 253–265.
- Wynn, R.B., Masson, D.G., Stow, D.A.V., Weaver, P.P.E., 2000b. Turbidity current sediment waves on the submarine slopes of the western Canary islands. *Marine Geology* 163 (1–4), 185–198.
- Wynn, R.B., Weaver, P.P.E., Masson, D.G., Stow, D.A.V., 2002. Turbidite depositional architecture across three interconnected deep-water basins on the north-west African margin. *Sedimentology* 49, 669–695.